1-1-2002

Stability properties of a formulation of Einstein's equations

Gioel Calabrese
Louisiana State University

Jorge Pullin
Louisiana State University

Olivier Sarbach
Louisiana State University

Manuel Tiglio
Louisiana State University

Recommended Citation

Calabrese, G., Pullin, J., Sarbach, O., & Tiglio, M. (2002). Stability properties of a formulation of Einstein's equations. *Physical Review D, 66* (6) https://doi.org/10.1103/PhysRevD.66.064011

Stability properties of a formulation of Einstein's equations

Gioel Calabrese,* Jorge Pullin,† Olivier Sarbach,‡ and Manuel Tiglio§
Department of Physics and Astronomy, Louisiana State University,
202 Nicholson Hall, Baton Rouge, Louisiana 70803-4001

We study the stability properties of the Kidder-Scheel-Teukolsky (KST) many-parameter formulation of Einstein's equations for weak gravitational waves on flat space-time from a continuum and numerical point of view. At the continuum, performing a linearized analysis of the equations around flat spacetime, it turns out that they have, essentially, no non-principal terms. As a consequence, in the weak field limit the stability properties of this formulation depend only on the level of hyperbolicity of the system. At the discrete level we present some simple one-dimensional simulations using the KST family. The goal is to analyze the type of instabilities that appear as one changes parameter values in the formulation. Lessons learnt in this analysis can be applied in other formulations with similar properties.

I. INTRODUCTION

Numerical simulations of the Einstein equations for situations of interest in the binary black hole problem do not run forever. The codes either stop due to the development of floating point overflows, or even if they do not crash, they produce answers that after a while are clearly incorrect. It is usually very difficult to pinpoint a clear reason why a code stops working. Recently, Kidder, Scheel and Teukolsky (KST) [1] introduced a twelve-parameter family of evolution equations for general relativity. Performing an empirical parameter study within a certain two-parameter subfamily, they were able to evolve single black hole spacetimes for over 1000 M, where M is the mass of the black hole, something that had been very difficult to achieve in the past. It is of interest to try to understand what makes some of the parameter choices better than others, in particular given that a twelve dimensional parameter study appears prohibitive at present. The intention of this paper is to take some steps in this direction. We will first perform a linearized analysis of the KST equations in the continuum, by considering small perturbations around flat space-time. We will observe that the stability of flat space-time is entirely characterized by the level of hyperbolicity of the system. Since the latter is controlled by the parameters of the family, this provides a first analytic guidance as to which values to choose. Unfortunately, the result is somewhat weak, since it just points to an obvious fact: formulations with higher level of hyperbolicity work better.

In the second part of the paper we perform a set of simple numerical tests. We consider spacetimes where all variables depend on one spatial coordinate, which we consider compactified for simplicity, and time. We are able to exhibit explicitly the various types of instabilities that arise in the system. Some of the results are surprising. For the situation where the system is weakly hyperbolic, the code is strictly non-convergent, but it might appear to converge for a significant range of resolutions. We will see that the addition of dissipation does not fix these problems, but actually can exacerbate them. It is often the case in numerical relativity that discretization schemes that are convergent for strongly hyperbolic equations are applied to weakly hyperbolic formulations. The examples of this section will teach us how dangerous such a practice is and confirm the analytic results of reference [2]. This part of the paper is also instructive in that the KST system has only been evolved with pseudo-spectral methods. We use ordinary integration via the method of lines.

The plan of this paper is as follows. In the next section we will discuss several notions of stability that are present in the literature, mostly to clarify the notation. In section III we discuss the stability of the KST equations in the continuum under linearized perturbations. In section IV we discuss the numerical simulations.

*Electronic address: gioel@lsu.edu
†Electronic address: pullin@lsu.edu
‡Electronic address: sarbach@phys.lsu.edu
§Electronic address: tiglio@lsu.edu

II. DIFFERENT DEFINITIONS OF STABILITY

The term *stability* is used in numerical relativity in several different ways. We therefore wanted to make the notation clear at least in what refers to this paper. Sometimes the notion of stability is used in a purely analytic context, while some other times it is used in a purely numerical one. Within analytical contexts, there are cases in which it is used to mean well posedness, as in the book of Kreiss and Lorenz [3]. In such a context well posedness means that the norm of the solution at a fixed time can be bounded by the norm of the initial data, with a bound that is valid for all initial data. In other cases it is intended to measure the growth of perturbations of a certain solution within a formulation of Einstein's equations, without special interest in whether the equations are well posed or not.

At the numerical level, a scheme is sometimes defined as stable if it satisfies a discrete version of well posedness. This is the sense in which stability (plus consistency) is equivalent to convergence via the Lax theorem [4]. Examples of this kind of instability are present in the Euler scheme, schemes with Courant factor that are too large, or other situations where the amplification factor (or its generalization) is bigger than one. Finally, the term stability has also historically been loosely used to mean that a simulation runs for a certain amount of time before crashing, or that the errors remain reasonably bounded as a function of time for a certain amount of time.

At the continuum, part of the problem we want to look at can then be stated as follows. Suppose there is a certain solution u_0 of Einstein's equations which is bounded for all times. One can prescribe the initial data f_0 that uniquely determines, through the use of the evolution equations, that solution. However, if one gives initial data slightly different from f_0, the corresponding solution might grow without bound or even blow up in a finite amount of time. This can happen either because this is the physical situation, or because the new solution u_1 does not satisfy the constraints, or does satisfy them but it is in a gauge that is becoming ill defined. Numerical simulations may blow up even when one tries to model physically stable spacetimes. This is the case for evolutions of Schwarzschild or Kerr black holes (which are known to be at least linearly stable with respect to physical perturbations.)

The time growth of solutions of a given set of partial differential equations can be classified according to whether or not it can be bounded by a time function that does not depend on the initial data. This leads to the concept of well posedness. Namely, a system of partial differential equations is said to be well posed at a solution $u_0(t)$ if there is a T and some norm such that

$$||u(t)|| \leq F(T)||u(0)|| \ \text{ for } 0 \leq t \leq T \tag{1}$$

for all solutions $u(t)$ with $u(0)$ sufficiently close to $u_0(0)$. For linear equations the bound can be tightened to an exponential, but for nonlinear systems $F(T)$ might be any other function that can even diverge at finite T. The strength of equation (1) characterizes the property that the bound is independent of the details of the initial data; in particular, of their frequency components. This is important in numerical simulations, where more (and higher) frequency components appear when resolution is increased. Well posedness is a necessary condition in order to have long term, convergent evolutions, but it is not sufficient. Indeed, the function $F(T)$ can grow quickly in time. In order to control $F(T)$ one has to go beyond well posedness and study non-principal terms. We will now apply these ideas to the KST equations.

III. THE KST FAMILY OF EQUATIONS AND THEIR LINEAR STABILITY

A. The formulation

Starting from the Arnowitt, Deser and Misner (ADM) equations, KST derive a family of strongly hyperbolic first-order evolution equations for the three-metric (g_{ij}), the extrinsic curvature (K_{ij}), and the spatial derivatives of the three-metric ($d_{kij} \equiv \partial_k g_{ij}$), which generalizes previous well posed formulations [5, 6]. A priori prescribing the densitized lapse $\exp(Q)$ as a function of spacetime, the lapse N is given by

$$N = g^{\sigma} e^{Q}, \tag{2}$$

where g is the determinant of the three-metric and σ a parameter. The shift vector, N^i, is also assumed to be prescribed as a function of spacetime. We define the derivative operator along the normal to the hypersurfaces as

$$\partial_0 = \frac{1}{N}(\partial_t - \pounds_{\vec{N}}).$$

The vacuum evolution equations have the form

$$\partial_0 g_{ij} \ = \ -2K_{ij}\,, \tag{3}$$

$$\partial_0 K_{ij} = -\frac{1}{2}\partial^k d_{kij} + \frac{1}{2}\partial^k d_{(ij)k} + \frac{1}{2} g^{ab}\partial_{(i} d_{|ab|j)} - \left(\frac{1}{2}+\sigma\right) g^{ab}\partial_{(i} d_{j)ab}$$
$$+ \zeta\, g^{ab} C_{a(ij)b} + \gamma\, g_{ij} C - e^{-Q}\partial_i\partial_j(e^Q) + \mathcal{R}_{ij}\,, \quad (4)$$
$$\partial_0 d_{kij} = -2\partial_k K_{ij} + \eta\, g_{k(i} C_{j)} + \chi\, g_{ij} C_k + \mathcal{R}_{kij}\,, \quad (5)$$

where the constraint variables

$$C = \tfrac{1}{2} g^{ab}\partial^k (d_{abk} - d_{kab}) + \mathcal{R}, \quad \text{(Hamiltonian constraint)}$$
$$C_j = \partial^a K_{aj} - g^{ab}\partial_j K_{ab} + \mathcal{R}_j, \quad \text{(momentum constraint)}$$
$$C_{kij} = d_{kij} - \partial_k g_{ij}\,, \quad \text{(definition of } d_{kij}\text{)}$$
$$C_{lkij} = \partial_{[l} d_{k]ij}\,. \quad \text{("closedness" of } d_{kij}\text{)}$$

have been added to the right-hand side of the evolution equations with some free parameteres $\zeta, \gamma, \eta, \chi$. Here, $\partial^k \equiv g^{kl}\partial_l$ and b_j, d_k are defined as the traces of d_{kij} :

$$b_j = g^{ki} d_{kij}\,, \quad d_k = g^{ij} d_{kij}\,.$$

The "remainder" terms $\mathcal{R}$, $\mathcal{R}_i$, $\mathcal{R}_{ij}$ and $\mathcal{R}_{kij}$ are homogeneous polynomials of degree 2 in d_{kij}, $\partial_i Q$ and K_{ij} (this will have direct consequences on the linear stability, as discussed below), where the coefficients may depend on g_{ij}. Finally, the Lie derivative of the symbols d_{kij} is

$$\pounds_{\vec{N}} d_{kij} = N^l\partial_l d_{kij} + d_{lij}\partial_k N^l + 2 d_{kl(i}\partial_{j)} N^l + 2 g_{l(i}\partial_{j)}\partial_k N^l.$$

The evolution system has characteristic speeds $\{0, \pm 1, \pm\sqrt{\lambda_1}, \pm\sqrt{\lambda_2}, \pm\sqrt{\lambda_3}\}$, where

$$\lambda_1 = 2\sigma,$$
$$\lambda_2 = 1 + \chi - \frac{1}{2}(1+\zeta)\eta + \gamma(2 - \eta + 2\chi),$$
$$\lambda_3 = \frac{1}{2}\chi + \frac{3}{8}(1-\zeta)\eta - \frac{1}{4}(1+2\sigma)(\eta + 3\chi).$$

It should be noted that these are the characteristic speeds with respect to the ∂_0 operator. This means that $\lambda = 0, 1$ correspond to propagation along the normal to the hypersurfaces or the light cone, respectively. The characteristic speeds μ with respect to the ∂_t operator are obtained from these after the transformation

$$\mu \mapsto N\mu + N^i n_i\,,$$

where n^i is the direction of the corresponding characterisitic mode.

The conditions under which the system is completely ill posed (CIP), weakly hyperbolic (WH) or strongly hyperbolic (SH) (see next subsection for these definitions) were found in KST. The system is CIP if any of the above speeds is complex, while it is WH if $\lambda_j \geq 0$ for $j = 1, 2, 3$ but one of the conditions (6, 7) below is violated. Finally, the system is SH provided that [7]

$$\lambda_j > 0, \quad \text{for } j = 1, 2, 3, \quad (6)$$
$$\lambda_3 = \frac{1}{4}(3\lambda_1 + 1) \quad \text{if } \lambda_1 = \lambda_2. \quad (7)$$

For example, if the parameters (ζ, γ, η, χ) are all zero the dynamics is equivalent to the ADM equations written in first order form with fixed densitized lapse and fixed shift (which are WH). If $\sigma = 0$ as well, then the system is equivalent to the ADM equations with fixed lapse and shift (which are also WH).

In KST seven extra parameters are introduced and used to make changes of variables in K_{ij} and d_{kij}. When performing this change of variables the constraint $C_{kij} = 0$ is also used in order to trade spatial derivatives of the three-metric for d_{kij}. Thus, the equations with the new variables have different solutions off the constraint surface. However, one can see that at the linear level this change of variables does not involve the addition of constraints.

B. Linear stability

Here we study the linear stability of the KST system considering perturbations of Minkowski spacetime written in Cartesian coordinates. That is, we assume that the background quantities are

$$g_{ij} = \delta_{ij}\,, \quad K_{ij} = 0, \quad d_{kij} = 0, \quad N^i = 0, \quad Q = 0.$$

In fact, since both Q and N^i can be freely specified, we will first fix them to their background values for simplicity (the more general case is analyzed at the end of this section.) Because the non-principal part of the evolution equations for K_{ij} and d_{kij} depends quadratically on K_{ij}, d_{kij} and the derivatives of Q, only the principal part remains when we linearize these evolution equations. More precisely, the linearized equations have the following structure:

$$\begin{aligned} \dot{g}_{ij} &= -2K_{ij}\,, \\ \dot{K}_{ij} &= (\boldsymbol{A}d)_{ij}\,, \\ \dot{d}_{kij} &= (\boldsymbol{B}K)_{kij}\,, \end{aligned} \tag{8}$$

where $\boldsymbol{A}$ and $\boldsymbol{B}$ are spatial, first order, differential linear operators with constant coefficients. Furthermore, perturbations of the three-metric do not appear in the equations for K_{ij} and d_{kij}. As a consequence, it is sufficient to consider only these equations; after having solved them, the three-metric is obtained through a time integration. So, the relevant linear evolution equations have the form

$$\dot{u} = \sum_{j=1}^{3} A^j \partial_j u\,, \tag{9}$$

where u is a "vector" formed by the components of K_{ij} and d_{kij} (u has, thus, 24 independent components); and A^j are 24×24 matrices.

Since the matrices A^j have constant coefficients and we want to make an analysis in the absence of boundaries, we consider a three-torus with periodic boundary conditions as a domain and analyze equation (9) through Fourier expansion. That is, we write

$$u(t,\vec{x}) = \sum_{\vec{k}} \hat{u}(t,\vec{k}) e^{i\vec{k}\cdot\vec{x}}\,.$$

The solution to equation (9) is, then

$$u(t,\vec{x}) = \sum_{\vec{k}} e^{iP(\vec{k})t} e^{i\vec{k}\cdot\vec{x}}\, \hat{u}(0,\vec{k})\,,$$

where $P(\vec{k})$, called the symbol, is defined by

$$P(\vec{k}) := \sum_{j=1}^{3} A^j k_j\,.$$

There are three different possibilities for the behavior of $e^{iP(\vec{k})t}$:

1. The system is SH: P has real eigenvalues and is diagonalizable, the solution simply oscillates in time. Nevertheless, we should keep in mind that the three-metric can grow linearly in time if $\vec{k} = \vec{0}$, see Eqs. (8). It is not difficult to see that this mode corresponds to an infinitesimal coordinate transformation.

2. The system is only WH: P has real eigenvalues but is not diagonalizable. Besides the zero-frequency growth in the metric, the Jordan blocks of dimension $n+1$ in P allow for growth in u that goes as $(kt)^n$, where $k = |\vec{k}|$.

3. The system is CIP: P has at least one complex eigenvalue. Besides the previous growing modes, there can be exponential —frequency dependent— growth, i.e. $u \approx \exp(\text{constant} \times kt)$.

To summarize, the linear stability properties of Minkowski spacetime depend only on the hyperbolicity of the system, since the non-principal terms are zero (except for the evolution equation for g_{ij}, but this equation decouples to linear order.) Stability advantages of the choice of parameters empirically found by KST in their analysis of a single black hole spacetime cannot be displayed in the example we have considered.

Finally, we study the effect of having a non-vanishing linearized (maybe densitized) lapse and shift: In this case, there are two extra terms in the evolution equation for K_{ij} and d_{kij}:

$$\begin{aligned} \dot{K}_{ij} &= (\boldsymbol{A}d)_{ij} - \partial_i\partial_j Q, \\ \dot{d}_{kij} &= (\boldsymbol{B}K)_{kij} + 2\partial_k \partial_{(i} N_{j)}. \end{aligned} \tag{10}$$

Since we assume that Q and N^i are prescribed, the solutions to these equations will have the form of the sum of a homogeneous solution and a particular solution. It is not difficult to find a particular solution, because we expect that a variation of Q and N^i induces an (infinitesimal) coordinate transformation $x^\mu \mapsto x^\mu + X^\mu$ with respect to which, in this case,

$$\begin{aligned} g_{ij} &\mapsto g_{ij} + 2\partial_{(i}X_{j)}, \\ K_{ij} &\mapsto K_{ij} - \partial_i\partial_j X^t\,, \\ d_{kij} &\mapsto d_{kij} + 2\partial_k\partial_{(i}X_{j)}. \end{aligned} \tag{11}$$

In fact, if we make the ansatz $K_{ij} = -\partial_i\partial_j f$, $d_{kij} = 2\partial_k\partial_{(i}\xi_{j)}$, we get a particular solution to the system (10) if

$$\begin{aligned} \dot{f} &= 2\sigma\partial^l\xi_l + Q, \\ \dot{\xi}_j &= \partial_j f + N_j\,. \end{aligned}$$

After a Fourier decomposition, this system has the form

$$\dot{v}(t,\vec{k}) = i\boldsymbol{M}(\vec{k})v(t,\vec{k}) + q(t,\vec{k}),$$

where v and q are formed by the Fourier amplitudes of f, ξ_j and Q, N_j, respectively ($j = 1\ldots3$), and

$$\boldsymbol{M}(\vec{k}) = \begin{pmatrix} 0 & 2\sigma k_1 & 2\sigma k_2 & 2\sigma k_3 \\ k_1 & 0 & 0 & 0 \\ k_2 & 0 & 0 & 0 \\ k_3 & 0 & 0 & 0 \end{pmatrix}.$$

By choosing the homogeneous solution to satisfy the appropriate initial data, it is enough to consider a particular solution with $v(t=0,\vec{k}) = 0$,

$$v(t,\vec{k}) = e^{i\boldsymbol{M}(\vec{k})t}\int_0^t e^{-i\boldsymbol{M}(\vec{k})s}q(s,\vec{k})ds.$$

If $\sigma > 0$ (as must be the case if the system is SH), the matrix $\boldsymbol{M}$ is diagonalizable, with real eigenvalues $0, \pm\sqrt{2\sigma|\vec{k}|^2}$. Since the norm of $\exp(i\boldsymbol{M}(\vec{k})t)$ can be bounded by a constant that does not depend on t nor on $\vec{k}$ (for example, if $2\sigma = 1$, the matrix $\boldsymbol{M}(\vec{k})$ is symmetric and $\exp(i\boldsymbol{M}(\vec{k})t)$ is unitary), this implies that v can grow at most linearly in time if q is uniformly bounded in time.

If v grows at most linearly in time, the same will hold for the main variables g_{ij}, K_{ij} and d_{kij}, see (11). Again, we do not see any dependence on the parameters found by KST in this particular example.

IV. NUMERICAL EXPERIMENTS

In [2] we show analytically that the iterated Crank–Nicholson (ICN) method with any number of iterations and the second-order Runge-Kutta methods do not yield convergent discretization schemes for systems of equations that are not strongly hyperbolic, even if dissipation is added. Here we exemplify this through the numerical evolution of the KST system in a simple situation. We evolve (3,4,5) in one dimension. That is, all quantities in those equations are assumed to depend only on t and x.

The sense in which stability is used in this section is that of the Lax equivalence theorem, i.e. a scheme is said to be stable if the numerical solution u_k^n at time $t = n\Delta t$ satisfies

$$||u^n|| \leq f(t)||u^0||$$

for all initial data u_k^0 and small enough Δt and Δx. Here the index n corresponds to the time step and k to the spatial mesh point. It is in this sense that stability plus consistency is equivalent, through Lax's theorem, to convergence (convergence with respect to the same discrete norm in which the scheme is stable and consistent). Note that in this context consistency means that the discrete equation approaches the continuum one in the limit of zero grid spacing. In what follows we use the discrete norm

$$||u^n||^2 = \sum_k \left(u_k^n\right)^2 \Delta x\,.$$

We will use second order Runge-Kutta (RK) for the time evolution. The spatial derivatives were discretized with centered differences, adding explicit lower order numerical dissipation as well, the amount of it being arbitrary. Most of the simulations presented here will be for RK, though the results are very similar for ICN (see the end of the section). In order to isolate our simulations from effects coming from boundary conditions, we will choose, as in Section III, periodic boundary conditions. Also, even though the analytic stability analysis of Section III and of Ref. [2] is linear, here we will present *nonlinear* simulations, but of situations that are close to flat spacetime. In all cases we will use the same initial data, same numerical scheme, and change only the continuum formulation of Einstein's equations.

Writing the evolution equations as

$$\dot{u} = Au' + l.o. \, ,$$

where "l.o." stands for lower order terms and time integration done with RK corresponds to

$$u_k^{n+1} = \left[1 + C\left(1 + \frac{C}{2}\right)\right] u_k^n \, , \tag{12}$$

where

$$C = \frac{A\lambda}{2}\delta_0 - I\tilde{\sigma}\lambda\delta^4 + \Delta t \times l.o. \, ,$$

with $\lambda = \Delta t/\Delta x$ the Courant factor, $\tilde{\sigma}$ the dissipation parameter and I the identity matrix, and

$$\delta_0 u_k = u_{k+1} - u_{k-1} \, , \tag{13}$$

$$\delta^4 u_k = u_{k+2} - 4u_{k+1} + 6u_k - 4u_{k-1} + u_{k-2} \, . \tag{14}$$

Our strategy for comparing numerical stability with the level of hyperbolicity is the following: we fix all parameters of the KST system except one, and change that single parameter in such a way that one gets a SH, WH or CIP system.

The metric that we evolve, giving the corresponding initial data, is

$$ds^2 = e^{f_1+f_2}(-dt^2 + dx^2) + dy^2 + dz^2 \, , \tag{15}$$

where $f_1 = f_1(t+x)$ and $f_2 = f_2(t-x)$ are arbitrary functions. This is an exact solution of Einstein's equations that is pure gauge, i.e. it is flat. In order to illustrate our point it is enough to make a simple choice for these functions, such as $f_1 = A\sin(x+t)$ and $f_2 = 0$ with $x \in [-\pi, \pi]$; furthermore, for the simulations shown below we choose $A = 0.01$.

A. Densitizing the lapse

A necessary condition in order to get well posedness within the KST system is to choose a positive densitization for the lapse, $\sigma > 0$. Furthermore, one has to take $\sigma = 1/2$ if one wants physical characteristic speeds. It is worth noticing that with $\sigma = 1/2$ and the metric (15), the perturbation in the densitization of the lapse Q is zero; thus, as shown in Section III, even off the constraint surface the solutions to SH formulations should only oscillate in time, except for possible zero-frequency linear growth.

In a similar way, choosing $\sigma = 0$ results in a WH system, and $\sigma < 0$ in a CIP one.

Densitizing the lapse is not enough for well posedness. One also has to add the constraints to the evolution equations. For definiteness, in this subsection we will show simulations using $\zeta = -1, \gamma = 0, \eta = 4, \chi = 0$ (which corresponds to the EC formulation without making the change of variables), but the main conclusions do not depend on this particular choice.

1. *The SH case ($\sigma = 1/2$)*

In order to understand some of the features of the SH numerical results that we will present we start analyzing, from a discrete point of view, the same numerical scheme when applied to the model equation

$$\dot{u} = u' \, . \tag{16}$$

Inserting the discrete Fourier mode

$$u_k^n = \hat{u}(\omega,\beta)e^{i(\omega n\Delta t+\beta k\Delta x)} \tag{17}$$

into the difference scheme (12), one obtains the discrete dispersion relation

$$e^{i\omega\Delta t} = 1+\left(i\lambda\sin(\beta\Delta x)-16S\sin^4\frac{\beta\Delta x}{2}\right)\left(1+i\frac{\lambda}{2}\sin(\beta\Delta x)-8S\sin^4\frac{\beta\Delta x}{2}\right)=\rho(\beta\Delta x)\,, \tag{18}$$

where $S=\tilde{\sigma}\lambda$. Equation (18) should be seen as a relation between ω and β. The discrete symbol, $\rho(\beta\Delta x)$ tells us how the different Fourier modes are damped and dispersed (see, e.g. [8], chapter 7). Writing $\omega=\alpha+ib$, we have that

$$e^{-b\Delta t} = |\rho(\beta\Delta x)|\,, \qquad \text{(amplification factor)} \tag{19}$$

$$\frac{\alpha}{\beta} = \frac{1}{\beta\Delta t}\arg(\rho(\beta\Delta x))\,. \qquad \text{(numerical speed)} \tag{20}$$

Choosing, for example, $\lambda=1/2$ and $S=0.01$, one can see [2] that the scheme (12) for Eq.(16) is stable and, therefore, convergent. From now on we will use, unless otherwise stated, these values. Figure 1 shows the magnitude of the amplification factor (19) and the numerical speed (20) for this choice of parameters.

The continuum equation (16) is neither dissipative nor dispersive. Ideally, one would like the difference scheme to have the same properties. For small values of A the initial data essentially consists of only one Fourier mode, $A\sin x$, which corresponds to $\beta=\pm1$. If one uses, say, 60 gridpoints and a spatial domain that extends from $-\pi$ to π, then one has that $\beta\Delta x=\pi/30$, for which Eq.(19) predicts a damping of about 0.0032% per crossing time. Similarly, from

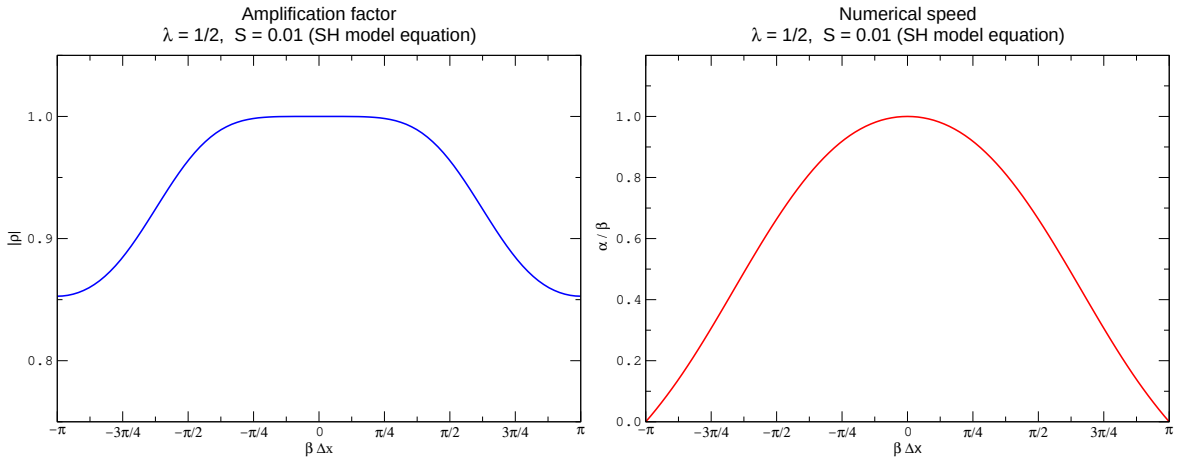

FIG. 1: Plot of the amplification factor and the numerical speed associated with difference scheme (12). If the product $\beta\Delta x$ is small enough, then the damping and the error in the propagation speed of the correspondent Fourier mode are very small.

Eq.(20) one can see that for this resolution and this initial data one should have a wave loss (i.e. the numerical and exact solution have a phase difference of 2π) at approximately $t=4,600$, which corresponds to 750 crossing times. Figure 2 show both the numerical and exact solution for the g_{xx} component of the metric at different times. The predicted speed difference is there and is in very good agreement with the analytical calculation based on the model equation. Also, the profile of the numerical solution maintains its shape for a very long time. Figure 3 shows the L_2 norm of the errors for this component at the same resolution. The errors come mostly from the speed difference, and the maxima and minima correspond to a phase difference between the analytical and numerical solution of odd and even multiples of π, respectively. Indeed, if one computes the error in the metric due to a phase difference of π, one gets

$$\left(\int_{-\pi}^{\pi}\left(e^{\sin(t+x)/100}-e^{\sin(t+x+\pi)/100}\right)^2dx\right)^{1/2}=0.035$$

which is in remarkable agreement as well with the maxima in figure 3. This speed difference is a rather usual numerical feature in solutions of finite difference schemes approximating hyperbolic equations. Usually this difference is *smaller* for bigger Courant factors [8], as can be seen from figure 4 for the particular discretization here used. One

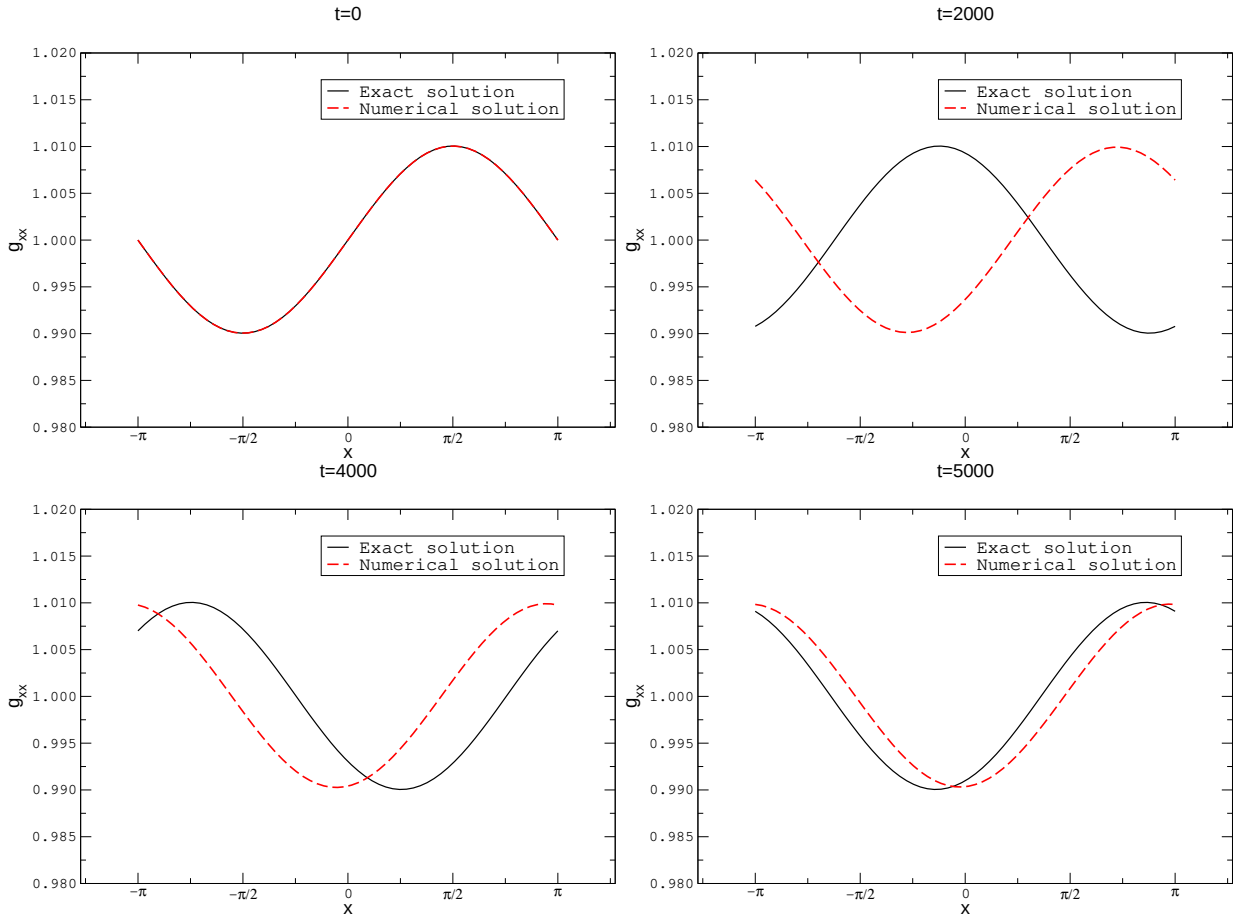

FIG. 2: Exact and numerical solutions for the SH case, at different times, showing the speed difference. This run was done with 60 grid points, $\lambda = 1/2$, $\tilde{\sigma} = 0.02$ and a domain of length 2π. With this resolution, the code 'loses' one wave after, roughly, 750 crossing times.

could try to push this factor to its stability limit, or use a different scheme that minimizes this effect. But here the point that we want to emphasize is that the errors in the SH simulation are second order convergent ones, as shown in figure 5. That figure shows the L_2 norm of the error in one component of the metric, g_{xx}, for resolutions ranging from 120 to 480 gridpoints, up to $1,000$ crossing times (in order to evolve up to $1,000$ crossing times without loosing a wave, one has to use more than 60 gridpoints). One can see that the errors grow linearly in time. One could be tempted to think that this is due to the zero-frequency linear mode predicted in Section III. This is not the case, in this simulation this mode is not excited (though it could be, in a more general evolution) and the error is caused by the numerical speed difference, as discussed above. Indeed, by performing a Fourier decomposition in space of the numerical solution one explicitly sees that the amplitudes are roughly constant in time (for non zero frequency components, this is exactly what the linearized analysis at the continuum predicted). Figure 6 shows some of these amplitudes for this simulation (to be contrasted later with the WH and CIP cases).

2. *The WH case ($\sigma = 0$)*

Figure 7 shows plots of the errors associated with evolutions performed with the same initial data, dissipation and Courant factor as above, except that now we densitize the lapse according to $\sigma = 0$ ("exact lapse"). For two fixed resolutions the coarsest one gives smaller errors after a while, and the time at which this occurs decreases as one increases resolution. This indicates that the difference scheme *is not convergent*. Note that one could be easily misleaded to think that the code is convergent if one did not evolve the system for long enough time, or without high enough resolution. For example, if one performs two runs, with 120 and 240 gridpoints, one has to evolve until, roughly, 150 crossing times, in order to notice the lack of convergence. To put these numbers in context, suppose one

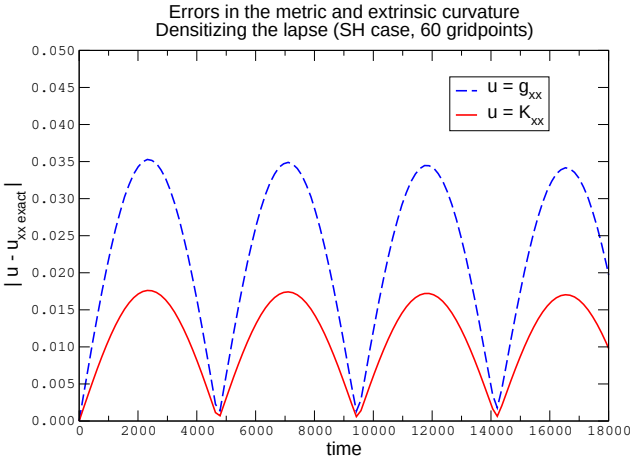

FIG. 3: L_2 norm of the errors for the metric and extrinsic curvature in the SH case. These errors are mostly from numerical speed difference, as described in the text.

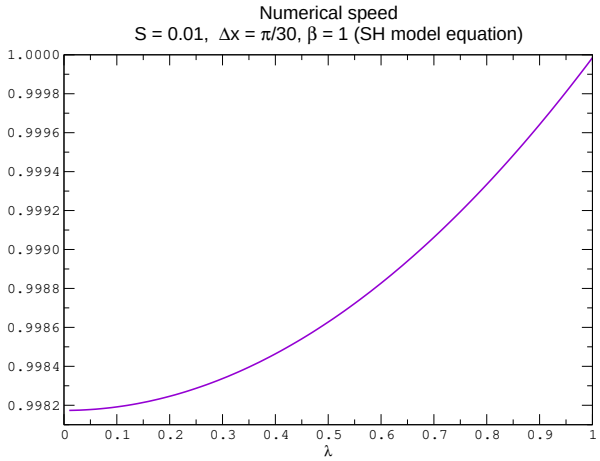

FIG. 4: Dependence of the numerical speed on the Courant factor. Increasing the Courant factor, decreases the error in the propagation speed.

had a similar situation in a 3D black hole evolution. To give some usual numbers, suppose the singularity is excised, with the inner boundary at, say, $r = M$, and the outer boundary is at $20M$ (which is quite a modest value if one wants to extract waveforms). In this case 120 and 240 gridpoints correspond to grid spacings of, approximately, $M/5$ and $M/10$, respectively (usual values as well in some simulations). If one had to evolve up to 150 crossing times in order to notice the lack of convergence, that would correspond to $t = 3,000M$, which is several times more than what present 3D evolutions last. Of course, the situation presented in this simple example need not appear in exactly the same way in an evolution of a different spacetime, or with a different discretization; in fact, in the next subsection we show an example where the instability becomes obvious sooner. Also, there are some ways of noticing in advance that the code is not converging. Namely, it seems that the numerical solution has the expected power law growth that the continuum linearized analysis predicts until all of a sudden an exponential growth appears. But if one looks at the Fourier components of the numerical solution, one finds that there are non-zero components growing exponentially from the very beginning, starting at the order of truncation error (see figure 8).

One might expect that, since for WH systems the frequency-dependent growth at the continuum is a power law one, it is possible to get convergence by adjusting the dissipation. In [2] we show that even though certain amount of dissipation might help, the code is never convergent and, indeed, adding too much dissipation violates the von Neumann condition, which leads to a much more severe numerical instability. We have systematically done numerical experiments changing the value of $\tilde{\sigma}$ without being able to stabilize the simulations (more details are given below), verifying, thus, the discrete predictions.

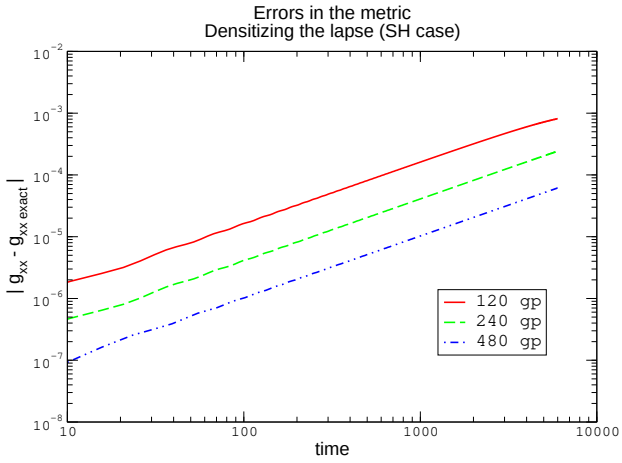

FIG. 5: L_2 norm of the errors for the metric.

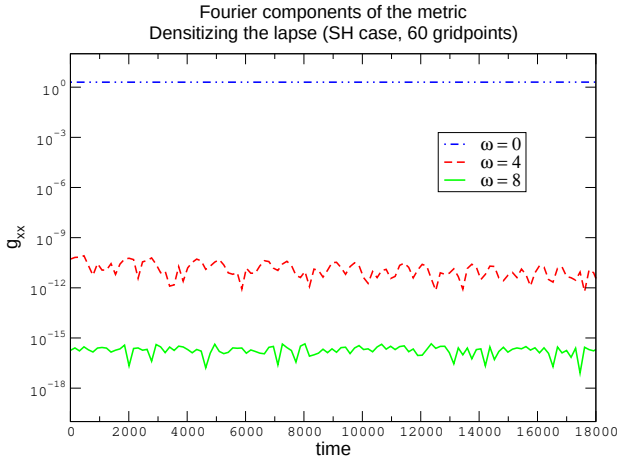

FIG. 6: Fourier components of the numerical metric for $\omega = 0, 4, 8$.

3. The CIP case ($\sigma = -1/2$)

Figure 9 shows the error in the metric, for different resolutions. As in the WH case, the errors originate mostly from the non-zero frequencies (i.e. the ones that typically grow in an unstable numerical scheme). But now they grow more than 10 orders of magnitude in much less than one crossing time and it is quite obvious that the code is not converging. This is so because in the CIP case the instability grows exponentially with the number of gridpoints. This can be seen performing a discrete analysis for the single ill posed equation in 1D, $v_t = iv_x$. One gets that the symbol $\rho(\beta\Delta x)$ is real and cannot be bounded by 1 in magnitude, making the difference scheme unstable (independently of resolution). If one changed to characteristic variables exactly this equation would appear in 1D as a subset of the system that we are considering, so this model equation is, in the linear approximation, part of the system evolved in this subsection. The amplification factor for this model equation is plotted in figure 11.

B. Adding the constraints

Now we fix all parameters except the one that corresponds to the addition of the Hamiltonian constraint, and choose three values that will render SH, WH and CIP systems. The results are very similar to those of the previous section, so we will present them in a less detailed way, except that now we will discuss the role of explicit dissipation.

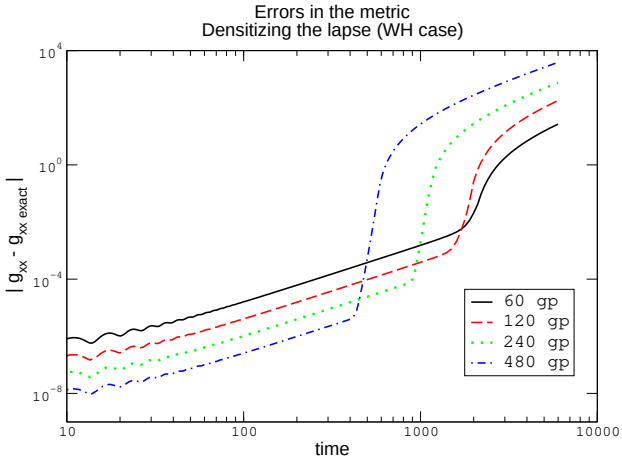

FIG. 7: L_2 norms of the errors for the metric.

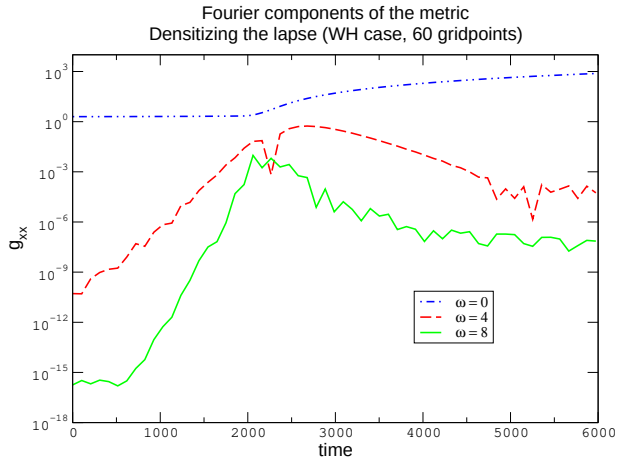

FIG. 8: Fourier components of the numerical metric for $\omega = 0, 4, 8$. Some of the components grow exponentially from the very beginning.

1. *The SH case*

We start by considering the one-parametric KST subfamily of strongly hyperbolic formulations of Eq.(2.39) of KST:

$$\sigma = \frac{1}{2}\,, \quad \zeta = -\frac{1}{9}(23 + 20\chi), \quad \gamma = -\frac{7}{6} \quad \eta = \frac{6}{5}\,. \tag{21}$$

This family has, for any value of χ, characteristic speeds 0 or ± 1 (see Section III), for the simulations here shown we chose $\chi = 1$ (and $\lambda = 1/2$, $\tilde{\sigma} = 0.02$, as in the SH simulations previously discussed). Figure 12 shows the analog of figure 5. As before, we do have convergence. The Fourier components of the solution remain constant in time, and the error comes mostly from the numerical speed difference.

2. *The WH case*

Here we also use the parameters given by (21) with $\chi = 1$, except that now we choose $\gamma = -32/21$. With this choice, $\lambda_1 = \lambda_3 = 1$, but $\lambda_2 = 0$; therefore, as summarized in Section III, the system is WH. As in the previous subsection, the difference scheme may appear to be convergent, but in fact it is not, see Figure 13. Frequency-dependent exponential growth starting at very small values accumulates and causes the instability. We have exhaustively experimented with different values for the numerical dissipation without being able to stabilize the code. Next we show some plots to

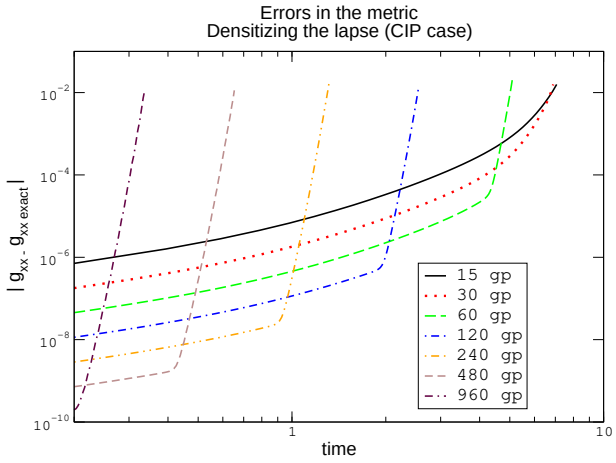

FIG. 9: L_2 norm of the errors for the metric.

illustrate this. In figure 14 we plot one of the Fourier components of the numerical metric. We increase the dissipation parameter $\tilde{\sigma}$, starting from $\tilde{\sigma} = 0.02$, and double it each time, while keeping the resolution and Courant factor fixed. At the beginning the rate of the exponential growth becomes smaller when one increases $\tilde{\sigma}$, though it is never completely suppressed, which causes the code to be non convergent. However, when one reaches the value $\tilde{\sigma} = 0.32$ the instability is even worse than adding less dissipation, and the same thing happens if one keeps on increasing $\tilde{\sigma}$ beyond 0.32. So we next narrow the interval in which the dissipation is fine tuned, we start at $\tilde{\sigma} = 0.24$, and increase at intervals of 0.01. We find the same result, at $\tilde{\sigma} > 0.25$ there is already too much dissipation and the situation is worse. Fine tuning even more, we change $\tilde{\sigma}$ in intervals of 0.001 around 0.250, but it is also found that for $\sigma > 0.250$ the effect of more dissipation is adverse, as also shown in figure 14.

The fact that beyond $\tilde{\sigma} = 0.250$ the situation becomes worse is in perfect agreement with the discrete analysis of [2]. There we show that a necessary condition for the von Neumann condition to be satisfied is $\tilde{\sigma}\lambda \leq 1/8$. Here the upper limit of 1/8 corresponds to, precisely, $\tilde{\sigma} = 1/4$. Exceeding this value results in a violation of the von Neumann condition; as explained in [2], when this happens there is a numerical instability that grows explonentially with the number of gridpoints (i.e. as in the CIP case), much faster than when the von Neumann condition is satisfied (in which case the growth goes as a power of the gridpoints).

Finally, it is worthwhile to point out that we have also tried with smaller Courant factors, using, in particular, values often used in numerical relativity, like $\lambda = 0.20$ and $\lambda = 0.25$, without ever being able to get a completely convergent simulation.

3. The CIP case

Finally here also use the parameters (21) with $\chi = 1$, but now we take $\gamma = -79/42$, which implies $\lambda_2 = -1$ and, thus, the system is CIP. The results are as expected. There is exponential, frequency-dependent growth that makes the numerical scheme unstable, see Figure 15.

C. Other simulations

Performing simulations with ICN instead of RK yields similar results, as predicted in [2]. Figure 16 shows, for example, evolutions changing the densitization of the lapse, as in the first subsection, but using ICN with two iterations (counting this number as in [9]). This is the minimum number of iterations that yields a stable scheme for well posed equations but, as shown in [2], it is unstable for WH systems. The same values of Courant factor and dissipation as above were used in these runs. We have also tried with other values of Courant factor and dissipation parameter, finding similar results. We were able to confirm the lack of convergence predicted in [2] in every WH or CIP formulation we used, including the ADM equations rewritten as first order equations in time space. Lack of convergence with a 3D code, using the ADM equations written as second order in space and ICN, for the same initial data used here, has also been confirmed [10].

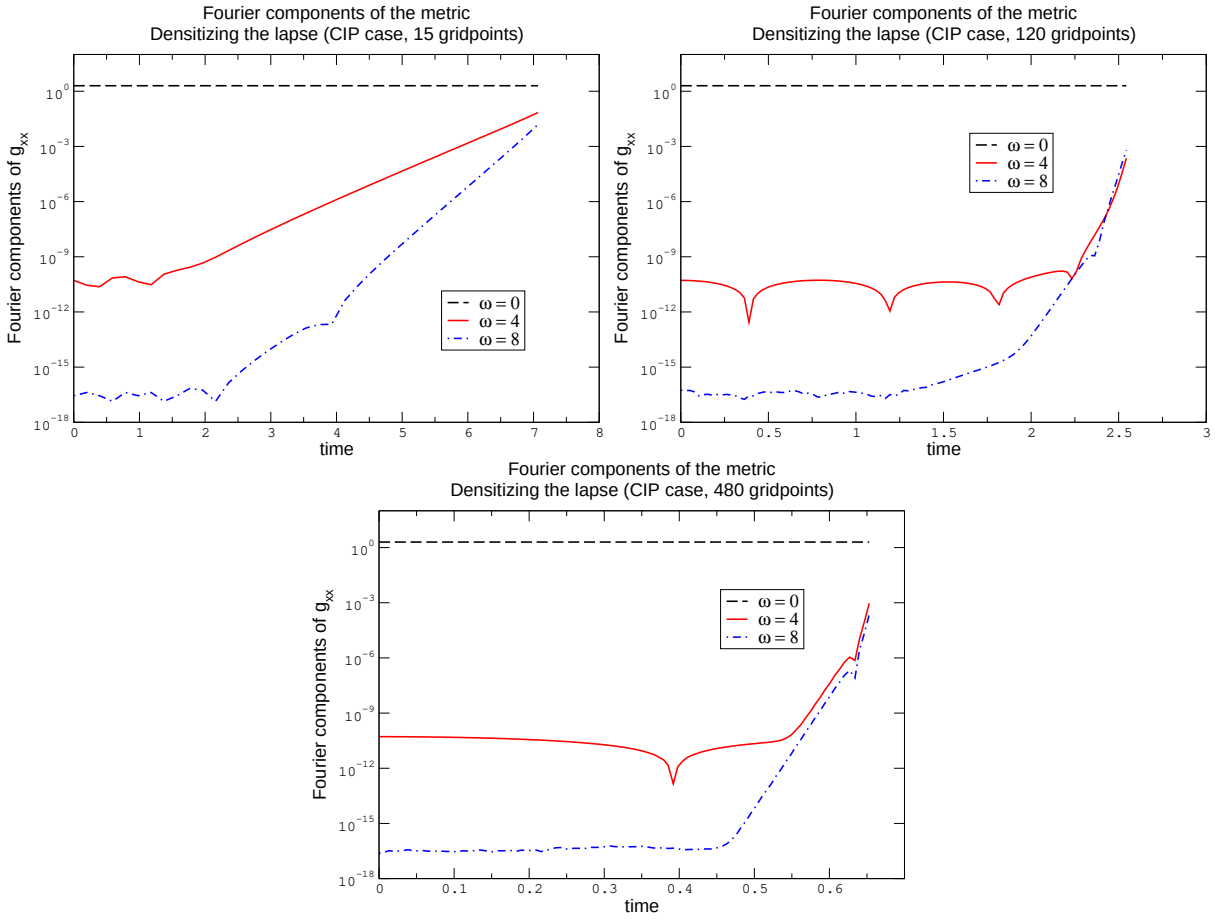

FIG. 10: The rate of growth of the Fourier components increases as one increases the resolution.

V. DISCUSSION

We have shown that a linearized analysis of the KST equations implies that flat space-time written in Cartesian coordinates is a stable solution of the equations if the parameters are chosen in such a way that the system is strongly hyperbolic. No further restrictions on the parameters are placed by this analysis. We have also integrated numerically the KST equations and shown that the system cannot be made stable (in the sense of Lax) and therefore convergent if the parameters are not chosen in such a way that the system is strongly hyperbolic. No amount of artificial viscosity was able to fix the problem.

The conclusions of Section III are, to some extent, similar to those of Alcubierre *et al.*, who find that, at the linearized level, the advantages of the Baumgarte–Shapiro–Shibata–Nakamura [11] with respect to the ADM formulation come from the fact that the first one is 'more' hyperbolic. However, since it is not 'completely' hyperbolic, an ill posed (zero speed, in the notation of [12]) mode is still present in BSSN. The conformal traceless (CT) decomposition is therefore introduced as a way of decoupling that mode. However, one could, instead, get rid of that mode by using a different choice of lapse. More explicitly, in the analysis of [12] exact lapse is used, but it is not difficult to see that choosing, for example, densitized lapse with, say, $\sigma = 1/2$, gets rid of the ill posed mode (indeed, certain version of BSSN with densitized lapse has been recently used in a 3D evolution of a single black hole [13]). Moreover, as shown in [14], the result is much stronger: even at the nonlinear level appropriately writing BSSN with densitized lapse results in a reduction (from first to second order in space) of certain strongly or symmetric hyperbolic formulations.

The lack of convergence in evolutions of WH or CIP systems with schemes that are convergent for well posed equations seems to have been overlooked in the past. If the von Neumann condition is satisfied, one could be easily misled to think that the scheme is convergent, especially if coarse resolutions are used, the evolution is short, or few frequencies are present in the initial data. Here we have shown that this lack of convergence does appear in concrete simulations, even in very simple ones. These numerical experiments, together with the theorem of reference [2] should be enough evidence to cast serious doubts on any simulation performed with evolution equations that are weakly

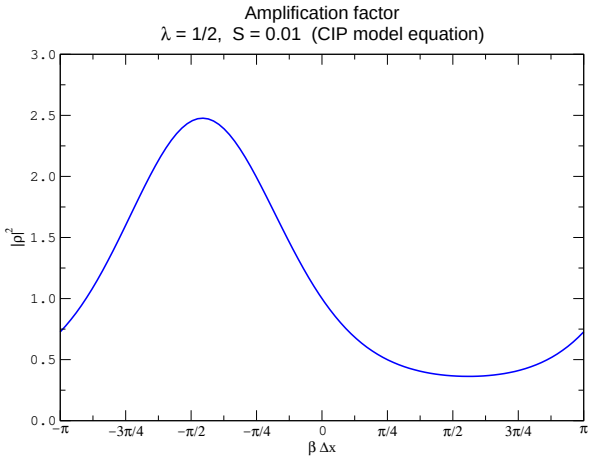

FIG. 11: Amplification factor associated with the difference scheme (12) approximating the ill posed equation $v_t = iv_x$.

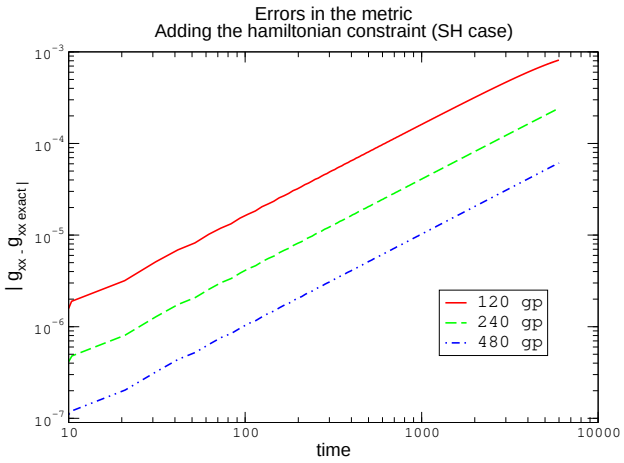

FIG. 12: L_2 norm of the errors for the metric.

hyperbolic that are not accompanied by very detailed convergence studies.

Summarizing, we do have analytical tools at our disposal to constrain schemes and predict to a certain extent their behavior under numerical evolution. In fact, the examples shown suggest that in the case of linearized equations, the analytical tools are complete: one can a priori tell if a code will work or not. In the non-linear case further tools will need to be developed to achieve the same status with respect to predicting the performance of a code before running it.

VI. ACKNOWLEDGMENTS

This work was supported in part by grants NSF-PHY-9800973, by funds from the Horace Hearne Jr. Institute for Theoretical Physics, by the Swiss National Science Foundation, and by Fundación Antorchas. We thank many interesting discussions with Larry Kidder, Saul Teukolsky, and Miguel Alcubierre. M.T. thanks Ed Seidel for hospitality at AEI, where part of this work was done.

[1] L.E. Kidder, M.A. Scheel, and S.A. Teukolsky, Phys. Rev. D **64**, 064017 (2001).
[2] G. Calabrese, J. Pullin, O. Sarbach, and M. Tiglio, *Convergence and stability in numerical relativity*, in preparation.

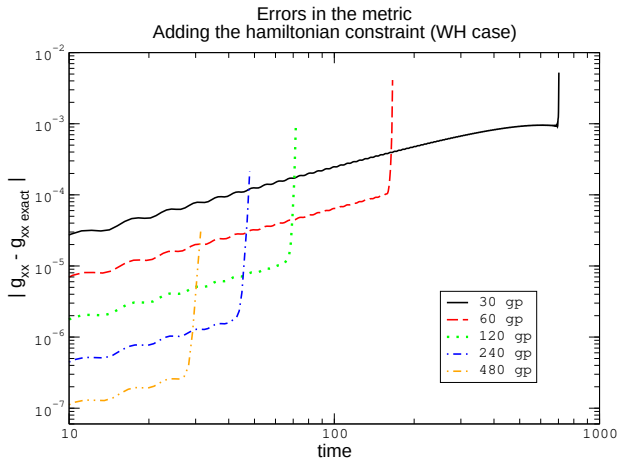

FIG. 13: L_2 norm of the errors for the metric. The simulation is stopped once the determinant of the spatial metric becomes zero.

[3] H.O. Kreiss, J. Lorenz, *Initial-Boundary Value Problems and the Navier-Stokes Equations* (Academic Press, 1989)

[4] R.D. Richtmyer and K.W. Morton, *Difference methods for initial-value problems*, (Krieger Publishing Company, Malabar, Florida, 1967)

[5] S. Frittelli and O.A. Reula, Phys. Rev. Lett. **76**, 4667 (1996); S. D. Hern, Ph.D. thesis, University of Cambridge, 1999, gr-qc 0004036.

[6] A. Anderson and J.W. York, Jr., Phys. Rev. Lett. **82**, 4384 (1999).

[7] O. Sarbach and M. Tiglio, in preparation.

[8] J.W. Thomas, *Numerical Partial Differential Equations, Vol I*, (Springer, New York, 1995),

[9] S.A. Teukolsky, Phys. Rev. D **61**, 087501 (2000).

[10] David Garrison, private communication.

[11] T.W. Baumgarte and S.L. Shapiro, Phys. Rev. D **59**, 024007 (1998); M. Shibata and T. Nakamura, Phys. Rev. D **52**, 5428 (1995).

[12] M. Alcubierre *et al.*, Phys. Rev. D **62**, 124011 (2000).

[13] P. Laguna and D. Shoemaker, gr-qc/0202105.

[14] G. Calabrese, J. Pullin, O. Sarbach, and M. Tiglio, gr-qc/0205064.

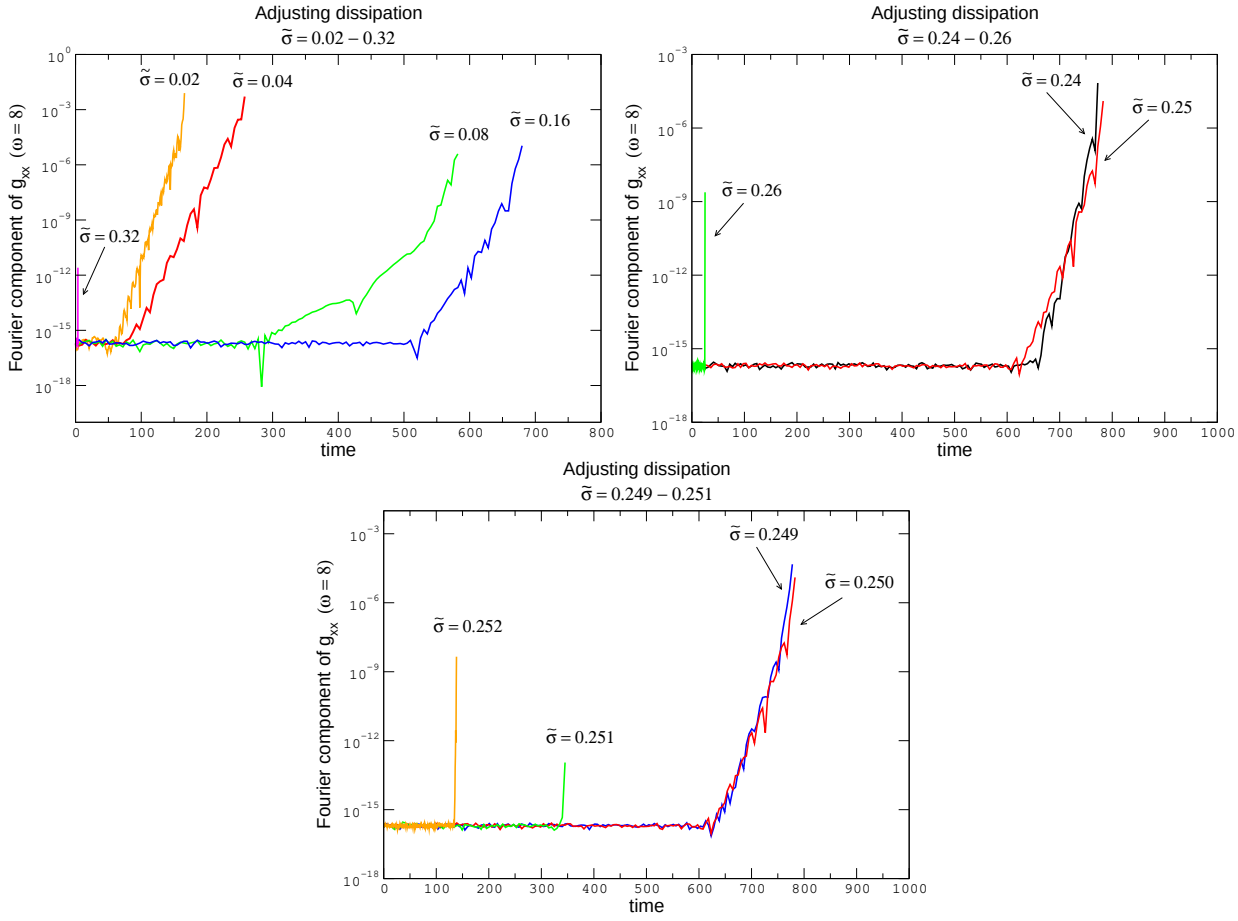

FIG. 14: We were not able to make the code stable by fine tuning the dissipation parameter.

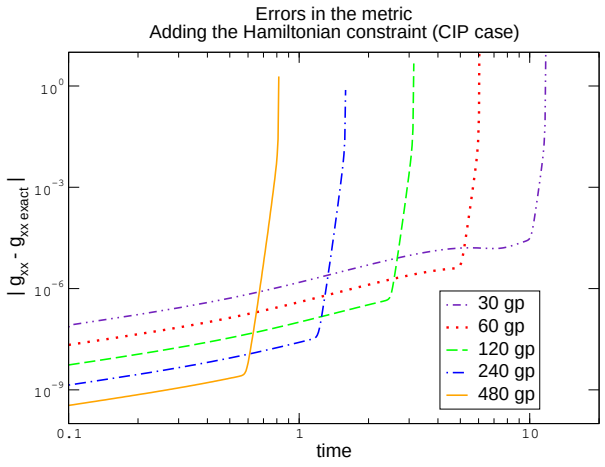

FIG. 15: L_2 norm of the errors for the metric.

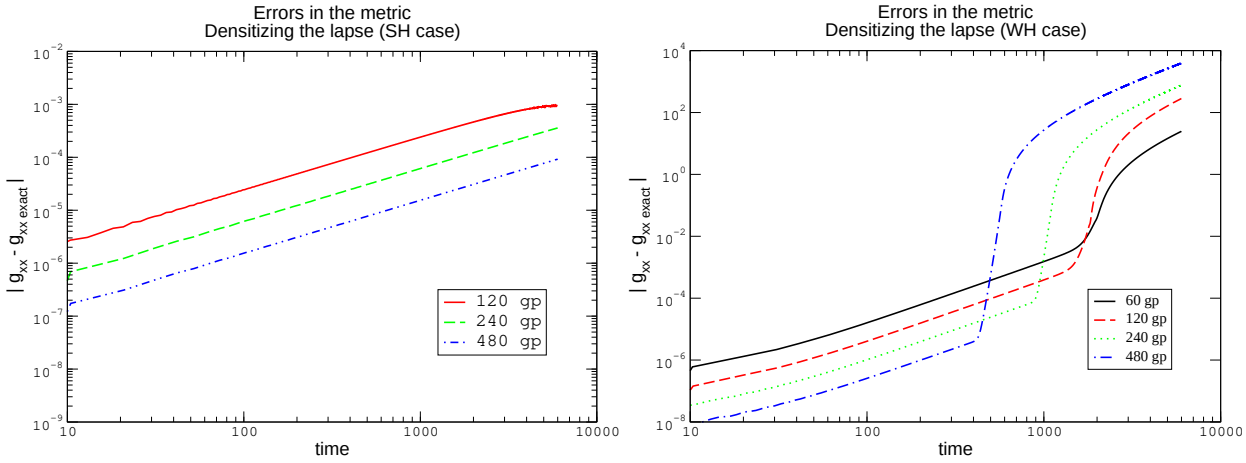

FIG. 16: L_2 norm of the errors for the metric using ICN.